Proceedings

Open-charm hadron measurements in Au+Au collisions at $\sqrt{s_{\mathrm{NN}}} = 200$ GeV by the STAR experiment†

Jan Vanek[1]*, *for the STAR Collaboration*

[1] Nuclear Physics Institute, Academy of Sciences of the Czech Republic; vanek@ujf.cas.cz
† Presented at Zimányi School 2018, Budapest, Hungary

Version August 14, 2019 submitted to Universe

Abstract: Study of the open-charm hadron production in heavy-ion collisions is crucial for understanding the properties of the Quark-Gluon Plasma. In these proceedings, we report on a selection of recent STAR measurements of open-charm hadrons in Au+Au collisions at $\sqrt{s_{\mathrm{NN}}} =$ 200 GeV, utilizing the Heavy-Flavor Tracker. In particular, the nuclear modification factors of D^0 and $\mathrm{D}^{\pm}$ mesons, elliptic and directed flow of D^0 mesons, Λ_c/D^0 and $\mathrm{D}_s/\mathrm{D}^0$ yield ratios are discussed.

Keywords: Quark-Gluon Plasma; open-charm hadrons; nuclear modification factor, elliptic flow, directed flow

1. Introduction

One of the main goals of the STAR experiment is to study the properties of the Quark-Gluon Plasma (QGP), which can be produced in ultra-relativistic heavy-ion collisions. Charm quarks are an excellent probe of the medium created in these collisions since they are produced predominantly in initial hard partonic scatterings and therefore experience the whole evolution of the medium.

As the charm quark propagates through the QGP, it interacts with the QGP and loses energy. The most common way to access the energy loss is by studying the modification of open-charm hadron yields in heavy-ion collisions with respect to those in p+p collisions using the nuclear modification factor:

$$R_{\mathrm{AA}}(p_{\mathrm{T}}) = \frac{\mathrm{d}N^{\mathrm{AA}}/\mathrm{d}p_{\mathrm{T}}}{\langle N_{\mathrm{coll}}\rangle \mathrm{d}N^{\mathrm{pp}}/\mathrm{d}p_{\mathrm{T}}}, \quad (1)$$

where $\langle N_{\mathrm{coll}}\rangle$ is the mean number of binary collisions, calculated using the Glauber model [1]. $R_{\mathrm{AA}} < 1$ for high-p_{T} open-charm hadrons is considered a signature connected with the presence of the QGP and the level of the suppression gives access to the strength of the interaction between the charm quark and the medium [2,3].

Another way to obtain information about the charm quark interaction with the QGP is to measure the azimuthal anisotropy of the produced charm hadrons (v_2). The magnitude of the v_2 that the charm quarks develop through the interaction with the surrounding medium carries important information about the transport properties of the medium [2,3].

To have a more complete picture of the open-charm hadron production in heavy-ion collisions, it is also important to understand the charm quark hadronization process. The charm quark hadronization mechanism can be studied through the measurements of the Λ_c/D^0 and $\mathrm{D}_s/\mathrm{D}^0$ yield ratios [4,5].

Since the charm quarks are created very early in the heavy-ion collisions, they can be used to probe initial conditions in such collisions. Recent theoretical calculations suggest that measurement of

the directed flow v_1 of open-charm mesons can be sensitive to the initial tilt of the QGP bulk and also to the initial electro-magnetic field induced by the passing spectators [6,7].

The following section summarizes recent STAR measurements of open-charm hadrons in the context of the observables and phenomena described above.

2. Open-charm measurements with the HFT

All results presented in this summary are from Au+Au collisions at $\sqrt{s_{\mathrm{NN}}} = 200$ GeV which were collected by the STAR experiment in years 2014 and 2016. Topological reconstruction of the decays, utilizing an excellent vertex position resolution from the Heavy-Flavor Tracker (HFT) [8], was used to extract the signals of the open-charm hadrons listed in table 1.

Table 1. List of open-charm hadrons measured using the HFT. The left column contains decay channels used for the reconstruction, $c\tau$ is the proper decay length of a given hadron, and BR is the branching ratio. Charge conjugate particles are measured as well. Values are taken from Ref. [9].

Decay channel	$c\tau$ [μm]	BR [%]
$\mathrm{D}^+ \to \mathrm{K}^-\pi^+\pi^+$	311.8 ± 2.1	9.46 ± 0.24
$\mathrm{D}^0 \to \mathrm{K}^-\pi^+$	122.9 ± 0.4	3.93 ± 0.04
$\mathrm{D}_\mathrm{s}^+ \to \phi\pi^+ \to \mathrm{K}^-\mathrm{K}^+\pi^+$	149.9 ± 2.1	2.27 ± 0.08
$\Lambda_c^+ \to \mathrm{K}^-\pi^+\mathrm{p}$	59.9 ± 1.8	6.35 ± 0.33

The reconstruction of $\mathrm{D}^\pm$ mesons in data from 2016 will be used as an example as the steps of reconstruction of all the aforementioned particles are similar. First, a series of selection criteria is applied to the events and tracks. Specific values of the criteria, used in the analysis of $\mathrm{D}^\pm$ mesons, are listed in table 2.

Table 2. Summary of selection criteria used for extraction of $\mathrm{D}^\pm$ candidates from the data. For more details, see the text.

Event selection		$\lvert V_\mathrm{z}\rvert < 6$ cm
		$\lvert V_\mathrm{z} - V_{\mathrm{z(VPD)}}\rvert < 3$ cm
Track selection		$p_\mathrm{T} > 500$ MeV
		$\lvert\eta\rvert < 1$
		nHitsFit > 20
		nHitsFit/nHitsMax > 0.52
		HFT tracks = PXL1 + PXL2 + (IST or SSD)
Particle identification	TPC	$\lvert \mathrm{n}\sigma_\pi\rvert < 3$
		$\lvert \mathrm{n}\sigma_\mathrm{K}\rvert < 2$
	TOF	$\lvert 1/\beta - 1/\beta_\pi\rvert < 0.03$
		$\lvert 1/\beta - 1/\beta_\mathrm{K}\rvert < 0.03$
Decay topology		$DCA_\mathrm{pair} < 80$ μm
		30 μm $< L_{\mathrm{D}^\pm} < 2\,000$ μm
		$\cos(\theta) > 0.998$
		$\Delta_\mathrm{max} < 200$ μm
		$DCA_{\pi-\mathrm{PV}} > 100$ μm
		$DCA_{\mathrm{K}-\mathrm{PV}} > 80$ μm

The events are selected so that the position of the primary vertex (PV) along the beam axis (V_z), which is determined using the HFT and Time Projection Chamber (TPC) [10], is no further than 6 cm from the center of the STAR detector. This is necessary due to physical dimensions and acceptance of the HFT. The value of V_z is also compared to that measured by the Vertex Position Detector [11] ($V_{\mathrm{z(VPD)}}$) which helps with rejection of pile-up events as the VPD is a fast detector.

From these events, only tracks with sufficiently large transverse momentum ($p_T > 300\,\mathrm{MeV}/c$) are selected to reduce the combinatorial background. The pseudorapidity criterion $|\eta| < 1$ is given by the STAR detector acceptance. All tracks are also required to have sufficient number of hits used for track reconstruction inside the TPC (nHitsFit) and to be properly matched to the HFT to ensure their good quality. In this case, a good HFT track is required to have one hit in each of the inner layers (PXL1 and PXL2) and at least one hit in one of the two outer layers (IST or SSD)[1].

Next, all the selected tracks are identified using the TPC and the Time Of Flight (TOF) [12] detectors. The particle identification (PID) with the TPC is done based on energy loss of charged particles in the TPC gas. The measured energy loss is compared to the expected one, which is calculated with Bichsel formula, using nσ variable [13]. The PID using TOF is done by comparing velocity of given particle measured by TOF (β) and that calculated from its momentum and rest mass (β_π or β_K).

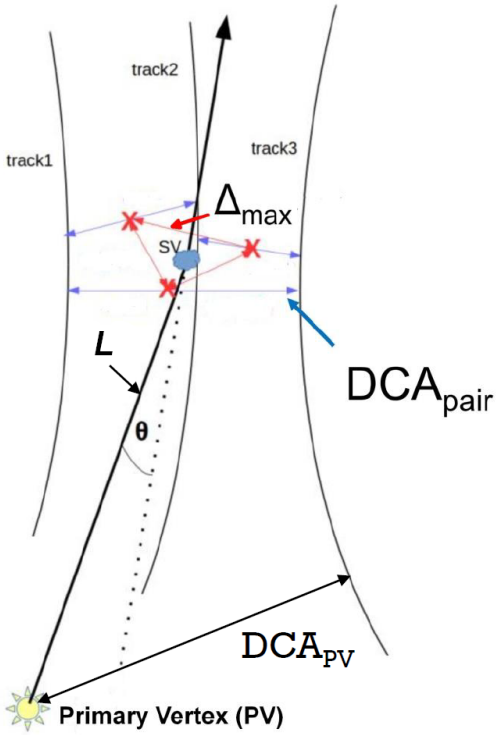

Figure 1. Depiction of a three body decay topology of $D^{\pm}$ mesons. For details about individual variables, see the text.

When charged pions and kaons are identified they are combined into K$\pi\pi$ triplets within each event. The topology of the triplet is then constrained using variables shown in figure 1. More specifically they are: the maximum distance of closest approach of track pairs (DCA_{pair}), $D^{\pm}$ meson decay length $L_{D^{\pm}}$, cosine of the pointing angle $\cos(\theta)$, maximum distance between reconstructed secondary vertices of track pairs (Δ_{max}), and the distance of closest approach to the primary vertex of the kaon (DCA_{K-PV}) and each of the pions ($DCA_{\pi-PV}$). Specific values used for $D^{\pm}$ result shown in figure 4 are listed in table 2. The topological selection criteria used for $D^{\pm}$ mesons will be optimized using the TMVA [14] in near future, as was done for other open-charm hadron results presented in the following section, in order to improve statistical significance and also to extend the p_T range.

[1] The HFT consists of total of four layers of silicon detectors. The two innermost layers are Monolithic Active Pixel Sensors (MAPS), PXL1 and PXL2. The outer layers are strip detectors, the Intermediate Silicon Tracker (IST) and the Silicon Strip Detector (SSD).

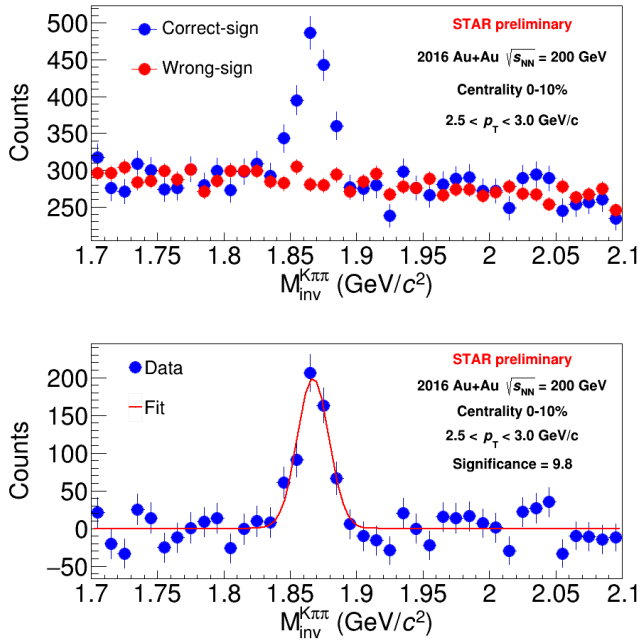

Figure 2. Invariant mass spectrum of Kππ triplets for: (**top**) correct-sign combinations (blue points) and with wrong-sign combinations (red points) and (**bottom**) after background subtraction. The data are fitted with Gaussian function.

The $D^{\pm}$ signal is subsequently extracted from the invariant mass spectrum of the Kππ triplets which are divided into two sets. The first consists of only correct-sign charge combinations, which may come from decay of $D^{\pm}$ mesons (see table 1) and contains the signal together with a combinatorial and a correlated background. The combinatorial background shape can be determined using the second set which contains only wrong-sign charge combinations which cannot originate from decay of $D^{\pm}$ mesons[2]. The correct-sign and the scaled[3] wrong-sign invariant mass spectrum of the Kππ triplets near invariant mass of the $D^{\pm}$ mesons is shown in top panel of figure 2. The scaled wrong-sign spectrum can be then subtracted from the correct-sign one which leads to the spectrum shown in the bottom panel of figure 2. The invariant mass peak is fitted with Gaussian function in order to determine its width σ and mean. The raw yield Y_{raw} is calculated using bin counting method in $\pm 3\sigma$ region around the peak mean.

[2] This method is sufficient for $D^{\pm}$ analysis. In case of e.g. D^0 or Λ_c, the correlated background needs to be addressed separately as it is more significant for those analyses.

[3] For combinatorial reasons, there are approximately three times as many wrong-sign charge combinations as the correct-sign ones in this case. The wrong-sign spectrum is therefore scaled so that it matches the correct-sign one in order to estimate the combinatorial background. The scale factor is determined from ratio of integrals of the correct and wrong-sign spectrum outside the $D^{\pm}$ mass peak region which is set $1.795\,\mathrm{GeV}/c^2 < M_{\mathrm{inv}} < 1.945\mathrm{GeV}/c^2$.

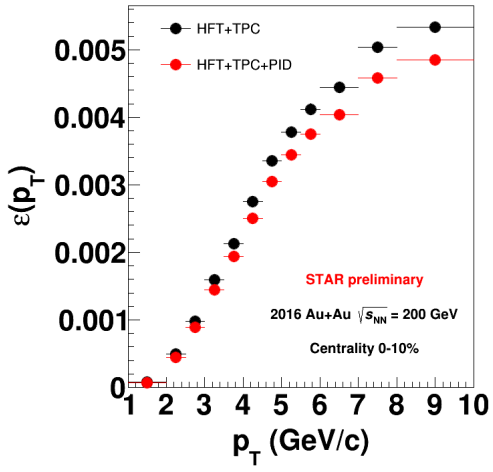

Figure 3. $D^{\pm}$ reconstruction efficiency in 0-10% central Au+Au collisions calculated using the data-driven fast simulator without (black points) and with the PID efficiency (red points).

The invariant spectrum of the $D^{\pm}$ mesons is then calculated from the raw yield $Y_{\rm raw}$ as:

$$\frac{d^2N}{2\pi p_T dp_T dy} = \frac{1}{2\pi p_T} \frac{Y_{\rm raw}}{N_{\rm evt} BR \Delta p_T \Delta y \varepsilon(p_T)}, \tag{2}$$

where $N_{\rm evt}$ is number of recorded MB events, BR is the branching ratio (see table 1) and $\varepsilon(p_T)$ is the total reconstruction efficiency calculated using the data-driven fast-simulator. More details about the efficiency calculation can be found in article [15]. An example of reconstruction efficiency of $D^{\pm}$ mesons in 0-10% central Au+Au collisions extracted with selection criteria from table 2 is shown in figure 3.

2.1. Results

Figure 4 shows the nuclear modification factor $R_{\rm AA}$ of D^0 [15] and $D^{\pm}$ mesons as a function of p_T in 0-10% central Au+Au collisions. Both D^0 and $D^{\pm}$ are significantly suppressed in high-p_T region which suggests a significant energy loss of charm quarks in the QGP. The low to intermediate p_T bump structure is consistent with predictions of models incorporating large collective flow of charm quarks [15].

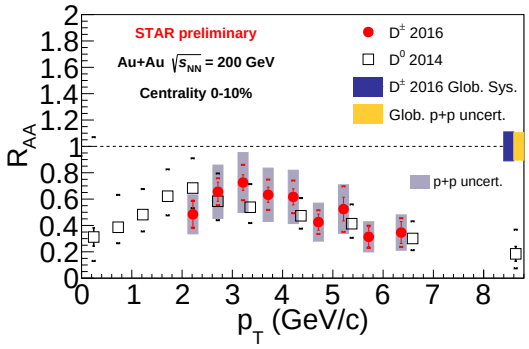

Figure 4. $R_{\rm AA}$ of D^0 [15] and $D^{\pm}$ mesons as a function p_T in 0-10% central Au+Au collisions at $\sqrt{s_{\rm NN}} = 200$ GeV. The p+p reference is from combined $D^{\star}$ and D^0 measurement by STAR in p+p collisions at $\sqrt{s} = 200$ GeV [16].

STAR has also measured and published the elliptic flow (v_2) of D^0 mesons using 2014 data [17]. Results with improved precision from the combined 2014+2016 data are shown in figure 5 (**a**). The

93 results clearly shows that charm quarks gain significant elliptic flow as they transverse through the
94 medium. It is also of importance to test the Number of Constituent Quarks (NCQ) scaling. In figure 5
95 (**b**) is shown the v_2/n_q as a function of $(m_T - m_0)/n_q$, where n_q is the number of constituent quarks,
96 m_T is the transverse mass and m_0 is the rest mass. In both panels, the D^0 results are compared to
97 similar measurements for light-flavor hadrons [18]. As can be seen in figure 5 (**b**), a similar scaling is
98 observed for all particle species within the uncertainties. The observation of sizable D^0 mesons flow
99 which follows the NCQ scaling, similarly as light-flavor hadrons, suggests that the charm quarks may
100 be in thermal equilibrium with the QGP at RHIC.

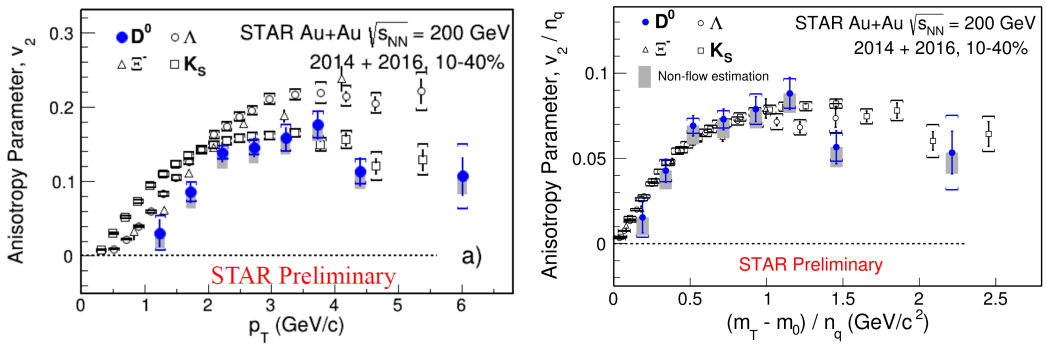

Figure 5. (**a**) The elliptic flow (v_2) of D^0 mesons and light-flavor hadrons [18] as a function of p_T. (**b**) The elliptic flow v_2 divided by the number of constituent quarks n_q as a function of $(m_T - m_0)/n_q$.

101 In order to study the charm hadronization and its possible modification in the presence of the
102 QGP, STAR has measured the Λ_c/D^0 yield ratio as a function of p_T and collision centrality, results
103 of which are shown in figure 6. As can be seen in panel (**a**), the ratio is significantly enhanced
104 compared to PYTHIA model predictions. The data are also compared to models that include coalesence
105 hadronization of charm quarks [4,5] which predict an enhancement of the ratio with a qualitatively
106 similar p_T dependence. The Λ_c/D^0 yield ratio increases from peripheral to central Au+Au collisions,
107 as shown in figure 6 (**b**). This and the qualitative agreement with the coalescence models indicates
108 that the Λ_c enhancement could be a consequence of coalescence hadronization of charm quarks in the
109 medium.

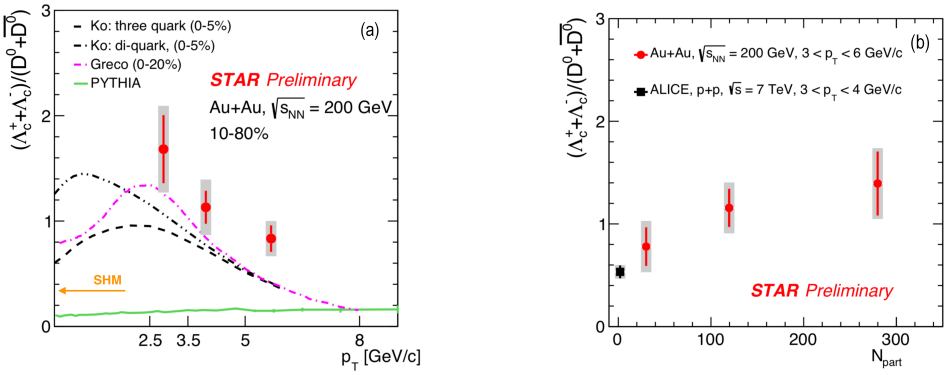

Figure 6. (**a**) The Λ_c/D^0 yield ratio as a function of p_T for 10-80% central Au+Au collisions at $\sqrt{s_{NN}} =$ 200 GeV. The data are compared to coalescence models [4,5], SHM [19] and PYTHIA. (**b**) The Λ_c/D^0 yield ratio as a function of centrality (red circles). The STAR data are compared to ALICE measurement for p+p collisions at $\sqrt{s} = 7$ TeV [20] (black square).

110 A complementary measurement to the one discussed above is the measurement of the D_s/D^0 ratio.
111 As shown in figure 7, the D_s is enhanced with respect to the averaged result from elementary collisions
112 [21] as well as PYTHIA model calculations. The TAMU model [22], which includes coalescence

hadronization of charm quarks, also shows an enhancement of the ratio, but underpredicts the data. This result also suggests that charm quarks hadronize via coalescence in heavy-ion collisions.

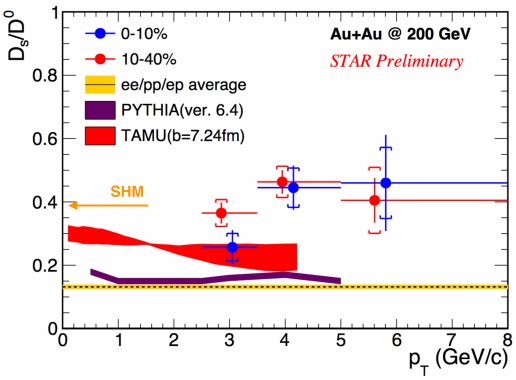

Figure 7. D_s/D^0 ratio as a function of p_T for two centralities. The data are compared to combined e+e, p+p and e+p data [21], PYTHIA, TAMU [22] and SHM [19] models.

The last result presented in these proceedings is from the measurement of (rapidity odd) directed flow (v_1) of D^0 mesons. There are two main models predicting the origin and magnitude of the v_1 of D^0 mesons. The first one is a hydrodynamical model which predicts larger v_1 slope (dv_1/dy) for heavy-flavor hadrons than for light-flavor hadrons, arising from a difference in the charm quark production profile and the tilted QGP bulk [6]. The second one calculates the v_1 from EM field induced by the passing spectators and predicts opposite v_1 slope for D^0 and $\overline{D^0}$ [7]. When combined, the prediction is that the v_1 slope for both D^0 and $\overline{D^0}$ mesons is negative, larger for D^0 than for $\overline{D^0}$, and much larger than for kaons [23]. As can be seen in figure 8, the measured slope of v_1 is indeed negative and larger in magnitude for both charmed mesons than for the light-flavor hadrons. On the other hand, the available statistics does not allow to firmly conclude on the D^0-$\overline{D^0}$ splitting.

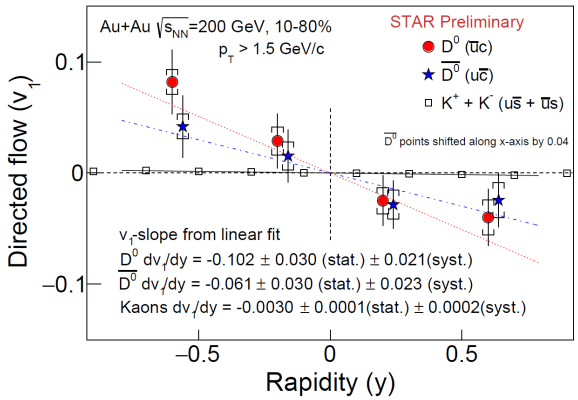

Figure 8. Directed flow of D^0 and $\overline{D^0}$ mesons as a function rapidity y in 10-80% central Au+Au collisions at $\sqrt{s_{NN}} = 200$ GeV. The data are compared to the similar measurement for charged kaons [24]. The solid black, dashed red and blue lines are linear fits to the data. Parameters of the fits are shown in the figure.

3. Summary

STAR experiment has extensively studied the open-charm hadron production utilizing the excellent vertex position resolution provided by the HFT. In this summary it is shown that D^0 and $D^{\pm}$ mesons are significantly suppressed in high p_T region which suggests strong interactions of the charm quarks with the QGP. The D^0 mesons also show large elliptic flow v_2 which follows the NCQ scaling, similarly as the light-flavor hadrons, suggesting that the charm quarks may be close to a local

thermal equilibrium with the QGP medium at RHIC. Moreover, the Λ_c/D^0 and D_s/D^0 yield ratios are found to be enhanced in Au+Au collisions. Comparison to model predictions suggests that the coalescence plays an important role in charm quark hadronization in heavy-ion collisions at RHIC. The measurement of the D^0 directed flow v_1 shows significantly larger values compared to those from light-flavor hadrons and is in qualitative agreement with hydrodynamic model predictions with a tilted QGP bulk [6]. The v_1 values for D^0 and $\overline{D^0}$ are consistent with each other within the current measurement precision.

Funding: These proceedings and presentation are supported by OPVVV grant CZ.02.1.01/0.0/0.0/16_013/0001569 of the Ministry of Education, Youth and Sports of the Czech Republic.

Acknowledgments: I would like to thank the organizers for giving me the opportunity to present STAR results at the Zimányi School 2018.

Conflicts of Interest: The author declares no conflict of interest.

References

1. M. L. Miller, *et al.*, Glauber Modeling in High Energy Nuclear Collisions, *Ann.Rev.Nucl.Part.Sci.*, **2007**, *57*, 205-243, doi: 10.1146/annurev.nucl.57.090506.123020.
2. S. Cao, *et al.*, Linearized Boltzmann transport model for jet propagation in the quark-gluon plasma: Heavy quark evolution, *Phys. Rev. C*, **2016**, *94*, 014909, doi:10.1103/PhysRevC.94.014909.
3. Y. Xu, *et al.*, Data-driven analysis for the temperature and momentum dependence of the heavy-quark diffusion coefficient in relativistic heavy-ion collisions, *Phys. Rev. C*, **2018**, *97*, 014907, doi:10.1103/PhysRevC.97.014907.
4. Y. Oh, *et al.*, Ratios of heavy baryons to heavy mesons in relativistic nucleus-nucleus collisions. *Phys. Rev. C*, **2009**, *79*, 044905, doi:10.1103/PhysRevC.79.044905.
5. S. Plumari, *et al.*, Charmed hadrons from coalescence plus fragmentation in relativistic nucleus-nucleus collisions at RHIC and LHC. *Eur. Phys. J. C*, **2018**, *78*, 348, doi:10.1140/epjc/s10052-018-5828-7.
6. S. Chatterjee and P. Bozek, Large Directed Flow of Open Charm Mesons Probes the Three-Dimensional Distribution of Matter in Heavy-Ion Collisions. *Phys. Rev. Lett.*, **2018**, *120*, 192301, doi:10.1103/PhysRevLett.120.192301.
7. S. Das, *et al.*, Directed flow of charm quarks as a witness of the initial strong magnetic field in ultra-relativistic heavy ion collisions, *Phys. Lett. B*, **2017**, *768*, 260, doi:10.1016/j.physletb.2017.02.046
8. D. Beavis, *et al.*, The STAR Heavy Flavor Tracker, Technical Design Report, **2011**.
9. M. Tanabashi, *et al.*, Review of Particle Physics, *Phys. Rev. Lett.*, **2018**, *98*, 030001, doi:10.1103/PhysRevD.98.030001.
10. M. Anderson, *et al.*, The STAR Time Projection Chamber: A Unique Tool for Studying High Multiplicity Events at RHIC, *Nucl.Instrum.Meth.A*, **2003**, *499*, 659, doi:10.1016/S0168-9002(02)01964-2.
11. W. J. Llope, *et al.*, The STAR Vertex Position Detector, *Nucl.Instrum.Meth.A*, **2014**, *759*, 23-28, doi:10.1016/j.nima.2014.04.080.
12. STAR TOF collaboration, Proposal for a Large Area Time of Flight System for STAR, May 24, **2004**.
13. M. Shao, *et al.*, Extensive Particle Identification with TPC and TOF at the STAR Experiment, *Nucl.Instrum.Meth.A*, **2006**, *558*, 419-429, doi:10.1016/j.nima.2005.11.251.
14. TMVA official website: http://tmva.sourceforge.net, (Accessed on: 23. 07. 2019).
15. J. Adam, *et al.*, Centrality and transverse momentum dependence of D^0-meson production at mid-rapidity in Au+Au collisions at $\sqrt{s_{NN}} = 200$ GeV, *Phys. Rev. C*, **2019**, *99*, 034908, doi:10.1103/PhysRevC.99.034908.
16. L. Adamczyk, *et al.*, Measuremets of D^0 and $D^\star$ production in p+p collisions at $\sqrt{s} = 200$ GeV, *Phys. Rev. D*, **2012**, *86*, 072013, doi:10.1103/PhysRevD.86.072013.
17. L. Adamczyk, *et al.*, Measurement of D^0 azimuthal anizothropy at midrapidity in Au+Au collisions at $\sqrt{s_{NN}} = 200$ GeV, *Phys. Rev. Lett.*, **2017**, *118*, 212301, doi:10.1103/PhysRevLett.118.212301.
18. B. I. Abelev, *et al.*, Centrality dependence of charged hadron and strange hadron elliptic flow from $\sqrt{s_{NN}} =$ 200 GeV Au+Au collisions, *Phys. Rev. C* **2008**, *77*, 054901 doi:10.1103/PhysRevC.77.054901
19. A. Andronic, *et al.*, Statistical hadronization of charm in heavy-ion collisions at SPS, RHIC and LHC, *Phys. Lett. B* **2003**, *571*, 36-44, doi:10.1016/j.physletb.2003.07.066.

20. S. Acharya, *et al.*, Λ_c^+ production in pp collisions at $\sqrt{s} = 7$ TeV and in p-Pb collisions at $\sqrt{s_{\rm NN}} = 5.02$ TeV, *J. High Energ. Phys.*, **2018**, *9*, 108, doi:10.1007/JHEP04(2018)108.
21. M. Lisovyi, *et al.*, Combined analysis of charm-quark fragmentation-function measurements. *Eur. Phys. J. C*, **2017**, *76*, 397, doi:10.1140/epjc/s10052-016-4246-y.
22. M. He, *et al.*, D_s Meson as a Quantitative Probe of Diffusion and Hadronization in Nuclear Collisions, *Phys. Rev. Lett.*, **2013**, *110*, 112301, doi:10.1103/PhysRevLett.110.112301.
23. S. Chatterjee and P. Bozek, Interplay of drag by hot matter and electromagnetic force on the directed flow of heavy quarks, arXiv:1804.04893.
24. L. Adamczyk, *et al.*, Beam-Energy Dependence of Directed Flow of Λ, $\overline{\Lambda}$, $K^{\pm}$, K_s^0, and ϕ in Au+Au Collisions, *Phys. Rev. Lett.*, **2018**, *120*, 062301, doi:10.1103/PhysRevLett.120.062301.